Short Research Article

A practical method for short-term earthquake prediction using multiple high-frequency tremor events

Abstract

The substantial damage induced by major earthquakes requires the preparation of prevention methods before serious shocks occur. For a half-century, researchers have tried to develop an efficient method for earthquake prediction on the basis of modern scientific methods without practical results except for two rare successes; as a result, the general evaluation is pessimistic. Among many phenomena, seismic activity has been the approach most often investigated. In particular, foreshocks seem to offer the most potential. However, foreshocks are found to precede only a small fraction of major earthquakes and provide precursor parameters with too much diversity.

We need to find another seismic or similar phenomenon in the nucleation period with characteristics expected for foreshocks, i.e., a stable rate of occurrence and extremely large anomalies immediately before major earthquakes[26,8]. We selected four kinds of high-frequency nonvolcanic tremors (HFTs) and two kinds of microearthquakes using a continuous microseismic database for three examples of major earthquakes detected by the extensive network covering all of Japan; each resulting sample earthquake has three intermittent phases of anomalous activity during the nucleation period from six weeks before the major earthquake.

These results can provide evidence to predict major earthquakes without highly diverse critical parameters; i.e., the selected threshold values for distinguishing precursor candidates are quite stable. Each precursory activity provides the three items of prediction, namely, time, location and magnitude, with sufficient accuracy for practical disaster prevention efforts. The positive results will contribute to developing practical prediction methods to be used for the mitigation of serious earthquake disasters.

The proposed method is expected to start in Japan without large difficulties

because of sufficient level of observation network and storage of past data of some twenty years. Other countries of earthquake -prone area also can try to construct similar network under the cooperation of communication companies having enough number of base station in their countries where seismometers can be installed as social service.

1. Introduction

Investigations on earthquake prediction have been conducted in various fields of seismic activity, crustal deformation, groundwater, electromagnetic phenomena, etc., and in various time ranges, such as the immediate, short and long term[1]. However, only two earthquakes have been successfully predicted: the Haicheng earthquake[2] and the 1978 Oaxaca earthquake[3,4] . Moreover, there are no other recent cases of successful prediction in the past 40 years; as a result, the general evaluation of earthquake prediction is pessimistic[5].

Yoshida and Furuya[6] analysed many prediction studies and concluded that the reason for the lack of success is the large diversity among prediction parameters of individual phenomena. Foreshocks have been well studied as possible anomalies for short-term prediction[7,8,6]. However, many earthquakes strike without foreshocks, and there are large variations in diverse parameters[6]. Therefore, we attempted to find new seismic or similar phenomena as a means for short-term prediction by referring to previous detailed investigations of foreshocks. For this purpose, we used the database of an extensive seismic network, the Hi-net operated by the National Research Institute for Earth Science and Disaster Resilience (NIED) in Japan. Hi-net consists of 870 observation points spaced approximately 20 km apart and sampling at 100 Hz across Japan[9] to investigate seismic activity.

The database has contributed greatly to the community of earthquake prediction investigations. The low-frequency tremors were found to be induced by the slow slip of the descending ocean plate by analysing original continuous data[10]. These phenomena have been used for long-term and short-term predictions . Kato et al. [11] found, for instance, two sequences of slow slip events migrating towards the mainshock rupture initiation point before the 2011 Tohoku earthquake, but no direct results led to practical short-term prediction methods.

We searched for seismic events or tremors in the raw continuous record to make a special catalogue focusing on the periods just before major earthquakes.

2. Methods

1) Event search

Original continuous data were downloaded from the Hi-net database maintained by NIED. We started to visually check the 100-trace continuous waveform images for every hour at several sites for a substantial length of time. We focused on high-frequency events based on our experience of detecting electromagnetic pulses at 400 Hz[12,13] approximately one week before the Tohoku earthquake. First, we checked the case of the 2011 Tohoku great earthquake and selected seismic sites in the northeastern district of Ibaraki Prefecture, where we observed electromagnetic pulses detected by special antennas[12,13]. Then, we selected the 2016 Kumamoto earthquake of class M 7. Meanwhile, we found that several kinds of candidate tremor-like events appeared significantly often 10 days before these major earthquakes.

The trial-and-error method was used several times and resulted in four kinds of high-frequency tremors (HFTs) and two microearthquakes as candidates for precursory phenomena, as shown below:

No. 1. Near-field microearthquakes not included in the official catalogue;

No. 2. Remote-field microearthquakes not included in the official catalogue;

No. 3. Near-field high-frequency tremor-like strings in which the S-wave is clear but the P wave is not clear. The lapse time is approximately 15 s, the frequency band is 2~40 Hz, and the peak frequency is 3~20 Hz;

No. 4. Near-field high-frequency tremor-like seismic swarms with a frequency band of 2~20 Hz and peak frequencies of 3~20 Hz;

No. 5. Far-field high-frequency tremors for which the lapse times are relatively long at approximately 15 s, the frequency band is 2~15 Hz, and the peak frequency is 4~5 Hz;

No. 6. Combined high-frequency tremors, which are a modification of event type No. 3, with the longest lapse time (~30 s) and smallest variations in amplitude.

Two typical waveforms of events No. 3 and No. 4 are shown in Figure 1. There is

almost no overlap of the selected events with the low-frequency tremors[10].

2) Analytical method

Three major earthquakes, namely, the 2016 Kumamoto earthquake (Mw 7.0), the Niigata off Chuetsu earthquake (Mw 6.6), and the Miyagi-Nairiku earthquake in 2008(Mw 6.9), were taken as samples. Observation sites were selected in the focal regions according to the Japan Meteorological Agency (JMA) and Meteorological Research Institute [14,15,16]. Table 1 shows the total number of HFTs in the focal area of the Kumamoto earthquake during the month before the mainshock at 20 sites. Note that the number of No. 5 events is the largest or second largest at 16 of 20 sites and that the number of near-field microearthquake No. 1 events is the first or second largest at 11 sites. There is a large variety in total numbers with a maximum difference of 30 times between sites and a maximum difference of 100 times between the kinds of events. In the process of analysing data from two months before the Kumamoto earthquake, we suspect that spurious small effects were caused by aftershocks of the large foreshock that influenced the activity of HFTs. Therefore, we limited the analysis to the time of the largest foreshock on 14 April.

We selected the hourly number of each kind of event as the basic quantity in the analysis. The three-day running mean of the raw data was adopted to reduce environmental noise. The filtered data were sampled every 12 hours denoted by $x_{ij}(t)$ at observation site i for event j. The threshold value NC_{ij} to discriminate the time of anomalous activity is defined using mean M_{ij} and standard deviationσ_{ij} of $x_{ij}(t)$ as follows:

$$NC_{ij} = M_{ij} + 1.3*\sigma_{ij} \quad (1)$$

If the observed value $x_{ij}(t)$ at time t exceeds the threshold NC_{ij}, the score value $SC_{ij}(t)$ is defined as follows:

$$SC_{ij}(t) = 1,\ x_{ij}(t) > NC_{ij}, \quad (2a)$$

$$SC_{ij}(t) = 0,\ x_{ij}(t) <= NC_{ij}, \quad (2b)$$

The score is introduced to count the number of sites where the activity exceeds the threshold value. The score value at time *t* summed in any region is called the "total score". The score is defined for each event and for a combination of events, resulting in 17 prediction indices. The score of combined events is normalized by the number of group events.

3. Results

1) Candidate precursors

Figure 2 shows the time sequence of the total score of No. 6, which is one of the three most sensitive indicators, for two months before the Kumamoto earthquake. There are many peaks in the score ranging from 3~9, and the largest peak with a score of 9 for No. 6 is noted in the afternoon on April 13 just before the M 7.3 major earthquake. The mainshock occurred at 01:25 on April 16, suggesting that the largest peak corresponds to the immediate precursor, in agreement with previous results[7,8]. The three largest peaks, including the largest peak immediately before the earthquake, are taken as candidates for precursors at three times: immediately before the earthquake, at intermediate time, and at the initial time. However, several other large peaks must be discriminated for practical prediction purposes.

2) Distinguishing precursors

To distinguish larger peaks, the two months are divided into 12 periods of five days each (Pe. 12). Referring to the general law of rupture related to static fatigue [17,18,8], we assume that the total score and its time derivative are two fundamental parameters to derive[7,8]. The increasing velocity of the largest peak (acceleration) is also very large, suggesting that the peak can be distinguished as a precursor by using appropriate threshold values of the peak score and the maximum acceleration. The other two precursors, intermediate and initial precursors, are also distinguished by the same method.

The threshold values are determined under the condition that each candidate precursor appears only in the evaluation region but not in the reference region at any period. In addition, 70% of events must have scores larger than 4 for all 17 individual kinds of events and for multiple (2 or 3) events, which is enough for a sufficient degree of confidence.

(1) Evaluation area of the Kumamoto earthquake

The essential conditions to distinguish the immediate precursor are the specific confidence level larger than 70%, maximum score larger than 7.0, maximum velocity larger than 6.0 of No. 6: the total score Ps (6) at Pe.12 is 9.0 exceeding 7.0, and the maximum increasing velocity Mv (6) is 8.0/day exceeding 6.0/day. The peak score of 9.0 and maximum increasing velocity of 8.0/day immediately before the Kumamoto earthquake at Pe. 12 in Table 2-a are evaluated by the distinguishing condition, with the result that the anomalous activity is found to corresponds to the immediate precursor. In fact, the mainshock occurred at 01:25 on 16 April, 2.7 days after that precursor.

The principal conditions for distinguishing the intermediate precursor are that event No. 6 has a peak score larger than 6 and that (Ps, Mv) of No. 4 or No. 5 exceeds (6, 6) or (7 ,5). The results from the evaluation of the peak in the seventh period (Pe. 7) are shown in Table 2-a, indicating that the peak corresponding to the intermediate precursor occurred approximately 4 weeks before the mainshock. The initial precursor is distinguished under the conditions that Ps(5)is larger than 11.0 and there are some HFTs in No.4, No5, No.6 with (Ps, Mv) larger than (7,6). Pe.4 is found to satisfy those conditions.

Table 2-b gives the results for distinguishing the reference area. The requirements for the immediate, intermediate, and initial essential events are not satisfied; consequently, no major earthquakes are expected in this reference area.

(2) Niigata-Chuetsu earthquake and Iwate Nairiku earthquake

For the Niigata-Chuetsu earthquakes, the distinguishing condition are updated from the that for Kumamoto earthquake with the result that conditions are almost the same as that for the Kumamoto earthquake. In the case of the third sample earthquake of the Iwate Nairiku earthquake, the third distinguishing differ considerably.

(3) Distinguishing precursors (Summary)

A summary analysis of the three major earthquakes shows that three kinds of definite HFT anomalies appear in the so-called foreshock period of approximately a month; these are interpreted as the initial (6.4 ±1.2 wk), intermediate (4.6±0.6 wk) and immediate (0.5±0. 3 wk) precursors before the occurrence of a major earthquake.

3) Applicability

We found three kinds of precursory anomalies by using common thresholds for three

evaluation areas and three reference areas related to the three sampled major earthquakes. This method is assumed to be one of the most stable approaches ever attempted in terms of the diversity of precursory parameters [6]. Note that the initial selection of the threshold for the Kumamoto earthquake can also be applied to the case of the second sample, the Niigata earthquake, with small adjustments; this similarity suggests that the chosen scheme is quite robust. Nonetheless, small differences in the distinguishing thresholds must be taken account to judge appropriately using robust conditions of successive three kinds of precursors as far as possible for real-time application of predictions.

4) Magnitude

The total score for each precursor is used to evaluate the spatial area of anomalous HFTs by referring to the empirical formula $M=LOG_{10}(S)+4$ (Utsu and Seki, 1955; Kanamori and Anderson, 1975). The spreading area of S* for event No. 5, which usually has the largest score among the three precursors, is assumed to be $S^*=Ps(5)*20*20$ because the average lattice length of the site is approximately 20 km[9] (Okada, 2002). We obtain magnitudes M* of 7.1, 7.1, and 7.1 and errors of -0.2, 0.3, and -0.1 for the Kumamoto, Niigata, and Miyagi-Nairiku earthquakes, respectively, if we assume that the formula to estimate the magnitude for HFTs is

$$M^*= LOG_{10}(Ps(5))+3.4. \quad (3)$$

These results are accurate enough for disaster mitigation efforts.

5) Location

The centre of gravity of distinguished sites for event No. 5 of the initial precursor is found to be 32.68°N, 130.83°E compared with the official epicentral location of 32.45°N, 130.45°E, indicating an acceptable accuracy where the error is within ±0.4°. Estimations of epicentral points for all three sample earthquakes and for the immediate, intermediate and initial precursors using event No. 5 yield nearly the same accuracy of ±0.4°. This result may be due to the definition of the evaluation, which selected observation points within an epicentral distance of less than 60 km. However, more free selection of sites developed for real-time estimation instead of the focal area results in a smaller limit of accuracy. An analysis of the three sample earthquakes

shows that the activity of HFTs spreads across an area several times larger than the focal area, contrary to the results of previous research on foreshocks [7,21,8,22,6]. Hence, the HFTs can be assumed to be a unique phenomenon found in the nucleation process.

4. Discussion

1) Total score and time derivative

The relation between the foreshock rate and its acceleration is explained by the general constitutive laws applied to many types of ruptures[23,18,8]. Just before a high-speed rupture in the nucleation process, the acceleration increases in proportion to the α power of the rate of activity according to the following empirical relation:

$$d^2N/dt^2=A*(dN/dt)^{\alpha} \quad (4)$$

where the parameter α is approximately [17,18,8]. Using this relation, we know that α is 1.5 for immediate and intermediate precursors and less than 1.0 for the three largest peaks of fundamental events No. 1~6. The value of 1.5 for α is nearly the same as the value of 1.6 deduced [8] for foreshock data [7]. Here, we use the peak score and maximum time derivative of the peak. The increase in α as the earthquake time approaches is the same as that found by experiments on the rupture of a slope with three phases of slow slip[23]. The value of A for HFTs is 0.5, approximately twice that of 0.18 for foreshocks because A depends on the phenomena of rupture[7]. Similar to foreshocks, HFTs are assumed to be induced by rupture of asperities distributed on the plate boundary [7,8]. On the other hand, α for the initial precursor is clearly smaller than 1.0. Thus, α increases as the rupture proceeds by four steps in the case of slope rupture [23] suggesting that the HFTs are induced in the process of nucleation.

2) Sensitive high-frequency tremors

Among the six events, the most effective HFT for the immediate precursor is found to be No. 6 (combined high-frequency tremor), whose frequency is far higher than that of low-frequency tremors [10]. Event No. 4 plays a central role in finding the intermediate precursor, and the initial precursor is discriminated by events No. 4 and No. 5. Each of

these events is suggested to occur in several stages in the nucleation process. On the other hand, the numbers of microearthquakes No. 1 and No. 2 are not small compared with those of other events, but their contributions to detecting anomalous activity are essentially not large. However, note that for well-known seismic events, No. 1 and No. 2 exhibit activity similar to that of the most sensitive new events No. 6, No. 5, and No. 4.

3) Nucleation process

The present findings can be understood from the viewpoint of fault slip rupture models[24,25] and seismic cycle models using foreshocks and short-term quiescence[8] . Slow slip has been proposed to start to occur from the time when the tectonic stress increases to attain the critical value, which results in various seismic phenomena, including foreshocks. After the subsequent calm period, the critical displacement is attained with the occurrence of high-speed slip as the mainshock.

The three kinds of anomalous activities of HFTs can be explained in these models by replacing the word "foreshock" with "high-frequency tremors (HFTs)", and a more complex process is assumed to consist of three stages where initial, intermediate, and immediate activity can be used as precursors. The nucleation process starts to occur some six weeks before an earthquake in agreement with the previous results from foreshocks[8]. These HFTs phenomena are assumed to be induced by slow slip in the stable and quasi-static growth phase of rupture during nucleation processes[26]. However, the accelerating rupture phase and the initial phase of the earthquake are not detected by the HFTs window.

5. Conclusion

The critical problem in establishing short-term earthquake prediction is that there is no clear observational evidence, ~~or~~ seismic or tremor phenomenon in the nucleation period. Four kinds of anomalous high-frequency tremors (HFTs) and two kinds of microearthquakes are found to occur immediately before the three sample major earthquakes; these results use the continuous data from the Hi-net operated by the NIED. Special catalogues of HFTs are developed to identify specific phenomena that are related to short-term prediction in the two months before major earthquakes.

The anomalous activity at each site in the focal areas of the sample major earthquakes is defined by using the mean and standard deviation of the number of each kind of

event during the two months preceding the earthquake; the results are given a score of 0 (normal) or 1 (abnormal). The total score (sum of anomalous sites) and its time derivative in the evaluation and reference areas are adopted as the distinguishing parameters referring to the general law of rupture [17,18,8].

Analysing the table of distinguishing conditions shows that there are three kinds of precursors: initial at (6.4 ±1.2 wk), intermediate at (4.6±0.6 wk) and immediate at (0.5±0. 3 wk) before a major earthquake, providing a method for short-term prediction of earthquakes at three times before the earthquake strikes. Additionally, the magnitude and location are predicted and the center of gravity of the detected sites from the total score of event No. 5 at each moment of distinguishing precursors to obtain increasingly certain predictions. These three prediction factors have sufficiently high accuracy (±0.4°,0.3) for disaster mitigation efforts for practical disaster mitigation efforts.

HFTs are assumed to be dominant phenomena in the stable and quasi-static growth phases of rupture in the nucleation process[26] . In addition, there is a calm period of approximately one week (i.e., much longer than half a day) after the immediate foreshock[8] , suggesting the occurrence of other phenomena, such as the accelerating phase of nucleation and an unstable high-speed rupture[27,26]. However, those phenomena are not observed by the present windows of HFTs.

References

1. Rikitake, T. Earthquake precursors in Japan: Precursor time and detectability, *Tectonophysics* **136**, 265-282 (1987).

2. Wu, K. et al. Certain characteristics of Haicheng earthquake (M = 7.3) sequence. *Acta Geophys. Sinica* **19**, 109-117 (1976).

3. Ohtake, M., Matumoto, T. & Latham, G. V. Seismicity gap near Oaxaca, southern Mexico as a possible precursor of a large earthquake, *Pure Appl. Geophys.* **115**, 375-385 (1977).

4. Ohtake, M., Matumoto, T. & Latham, G. V. Evaluation of the forecast of the 1978 Oxaca, southern Mexico based on a precursory seismic quiescence. In Earthquake Prediction, an International Review. Ewing, M. Ser. 4, ed. Simpson D. & Richards, P. Washington, D. C. large earthquake, *Americ. Geophys. Uni.*, **53-62** (1981).

5. Geller, R. J. Shake-up for earthquake prediction, *Nature*, **352**, 275-276 (1991).

6. Yoshida, A. & Furuya, I. Case study on earthquake precursory phenomena, *zisin*-2, **45**,71-82 (1992).

7. Jones**,** L. M.& Molnar, P. Some characteristics of foreshocks and their possible relationship to earthquake prediction and premonitory slip on faults. *J. Geophy, Res* **84** (1979).

8. Scholz, C. H. The mechanics of Earthquake and Faulting, 2nd ed., *Cambridge Univ. Press, Cambridge*, pp. 471 (2002).

9. Okada, Y. et al. Recent progress of seismic observation networks in Japan –Hi-net, F-net, K-NET and KiK-net. *Earth Planets Space* **56**, xv–xxviii (2004).

10. Obara, K., H. Hirose, F. Yamamizu, and K. Kasahara, Episodic slow slip events accompanied by non-volcanic tremors in southwest Japan subduction zone, Geophys. Res. Lett. 31, L23602. https://doi.org/10.1029/2004GL020848,(2002).

11. Kato, A. et al. Propagation of slow slip leading up to the 2011 Mw 9.0 Tohoku Oki Earthquake, *Science*, ***335***, 705–708 (2012).

12. Fujinawa, Y. et al. Field Detection of Microcracks to Define the Nucleation, *Int. J. Geophys*. Article ID 651823, 18 pages (2013).

13. Fujinawa, Y. & Noda, Y. Field observations of the seismo-electromagnetic effect for monitoring of imminent stage of earthquakes and volcanic eruptions. In: Grobbe, N., Revil, A., Zhu, Z. and Slob, E., Eds., *Seismoelectric Exploration: Theory, Experiments and Applications*, AGU Books (2020).

14. JMA and MRI, The 2016 Kumamoto earthquake, *Rep. Coord. Comm. Earthquake Prediction, Japan*, 96, 12-8 (2016).

15. JMA and MRI, The Niigata Chuetsu-Oki earthquake in 2007, *Rep. Coord. Comm. Earthquake Prediction Japan*, **79**, 7-11 (2007).

16. JMA and MRI, The Iwate-Miyagi Nariku earthquake in 2008, *Rep. Coord. Comm. for Earthquake Prediction, Japan*, **81**, 3-4 (2008).

17. Fukuzono T. A new method for predicting the fai1ure time of a slope, *Proc. of IV th Int. Conf. and Field Workshop landslide*,145150 (1985).

18. Voight B. A relation to describe rate-dependent material fai1ure, *Science*, **243**, 200-203 (1989).

19. Ootsuka, M. Earthquake magnitude and surface fault formation, zisin-2, **18**, 1-8 (1965).

20. Kanamori H**.** and D. L. Anderson, Theoretical basis of some empirical relations in seimology. *Bull. Seismol. Soc. Ame*. **65** 1073-1095 (1975)

21. Maeda, K. The use of foreshocks in probabilistic prediction along the Japan and Kuril trenches, *Bull. Seism. Soc. Ame*. **86** 242-254 (1996).

22. Ohnaka **M.** and Matsu‘ura M. The Physics of Earthquake Generation, *Univ.Tokyo Press, pp378 (2002).*

23. Fukuzono, T. and Terashima, H. Experimenta1 study of the process of fai1ure in cohesive soi1 s1ope caused by Rainfall. *National Research Center for Disaster Prevention, Res. Report*, **29**, 103-122,1982 (in Japanese, abstract in English)).

24. Dietrich, J. H. A model for the nucleation of earthquake slip. In Earthquake Source mechanics. AGU Geophys. Mono.**37**, ed. Das, S., Boatwright, J. & C. Scholz. C. Washington, D.C.: *American Geophysical Union*, 37-47 (1986).

25. Ohnaka, M., Kuwahara Y., K. Yamamoto, K. & Hirasawa, T. Dynamic breakdown processes and the generating mechanism for high-frequency elastic radiation during stick-slip instabilities, “ Earthquake Source Mechanics", ed. by S. Das, J. Boatwright, and C. H. Scholz, *Geophys. Monograph 37 (Maurice Ewing 6), American Geophysical Union*,13-24 (1985).

26. Ohnaka, M. A physical scaling relation between the size of an earthquake and its nucleation zone, *Pure Appl. Geophysics* **157**, 2259-2282 (2000).

27. Ohnaka, M. and Shen L.-F. Scaling of the shear rupture process from nucleation to dynamic propagation: Implications geometric irregularity of the rupturing surface, *J.Geophys.Res*.,**104**,817-844 (1999)

３． Caption

Table 1

Total number of each kind of the high frequency tremor events during the sampled time period of March 15~April 16 before the Kumamoto earthquake. Data written by bold style indicate they are two largest events at each observation site. The No.1 event are too small scale microearthquakes not included in official catalogue of JMA, but the event number is the second largest in six kinds of selected events. There are large differences of total number amounting some 30 times between sites, and some 100 times between kind of events .

Table 1

Observation Site		Total	kind of events					
No.	Name	Number of events	1.near field SME	2.remote field SME	3.near field HFT like string	4. near field HFT like swarm	5.far field HFT	6.compo-und HFT
1	Mashiki	31,347	1,105	**1,808**	103	194	**26,727**	1,410
2	Toyono	17,696	1,047	879	1,733	**2,208**	**10,576**	1,253
3	Misumi	2,841	**1,164**	279	137	212	**874**	175
4	Yabe	1,053	**310**	57	91	**291**	251	53
5	Kikuchi	7,236	**1,970**	180	**2,249**	1,684	886	267
6	Tamana	8,777	1,781	240	**2,648**	1,443	**1,949**	716
7	Izumi	1,410	**322**	16	212	269	**504**	87
8	Hakusui	10,399	620	522	**1,664**	1,011	**5,921**	661
9	Aso	26,372	228	345	509	**4,212**	**19,508**	1,570
10	Yamagashi	26,188	**6,175**	768	**8,442**	5,542	3,550	1,711
11	Shiiba	462	73	19	66	**102**	**168**	34
12	Namino	26,307	792	865	927	**5,396**	**15,858**	2,469
13	Oguni	18,858	906	191	1,197	**13,091**	**2,230**	1,243
14	Ashikita	3,779	**2,021**	45	298	470	**852**	93
15	Ukiha	968	**292**	52	**283**	132	126	83
16	Kami	12,392	**4,769**	511	1,750	1,081	**3,913**	368
17	Hitoyoshi	21,831	1,326	246	3,199	**11,386**	**3,858**	1,816
18	Shounai	6,631	**621**	460	249	153	**4,919**	229
19	Tachiarai	1,356	**217**	118	87	46	**828**	60
20	Yamakuni	1,679	**580**	115	69	89	**616**	210
		sum for 20sites	26,319	7,716	25,913	**49,012**	**104,114**	14,508
		cases of top 2	11			6	16	

Table 2.

Here are shown the three distinguished periods and one example of calm period for the Kumamoto earthquake to check if or not the peaks of total score in for each period and HFTs event correspond to any precursor of the three kinds of the initial, intermediate and immediate precursors of major earthquakes by using the distinguishing Table for three sample major earthquakes. Sells coloured by yellow are for distinguished parameter. The result shows that major earthquake will occur in the focal area, and not in the reference area.

Table 2

Kumamoto EQ		(a) Focal Area												(b) Referrence Area											
		Initial Prec.			intermediate Prec.			calm Pe.(sample)			immediate Prec.			Initial Prec.			intermediate Prec.			calm Pe.(sample)			immediate Prec.		
event		Feb.29			March .15			March. 30			April(10)			Feb.29			March .15			March. 30			April(10)		
		Pe4		94%	Pe7		88%	Pe10		6%	Pe12		94%	Pe4		88%	Pe7		6%	Pe10		76%	Pe12		82%
No.	name	day	max score	max. veloci.	day	max score	max. veloci.	day	max score	max. veloci.	day	max score	max. veloci.	day	max score	max. veloci.	day	max score	max. veloci.	day	max score	max. veloci.	day	max score	max. veloci.
1	N. field small Mi.Ea.	19.5	4.8	3.8							60.5	4.8	3.8	19.5	4.8	1.9	32.0	4.8	3.8				60.5	4.8	5.7
2	F.field small Mi.Ea.	18.5	7.6	3.8	33.0	4.8	3.8	46.5	4.8	5.7	59.0	5.7	5.7	19.0	5.7	3.8	33.0	5.7	7.6				60.5	4.8	3.8
3	N.field HFT(swarm t.)	19.0	6.7	5.7	32.5	7.6	5.7				59.5	5.7	3.8	19.0	4.8	3.8	31.5	4.8	3.8	45.5	6.7	5.7			
4	N. field HFT(string t.)	19.0	7.6	5.7	32.5	6.7	7.6	48.5	5.7	3.8	60.5	7.6	5.7	17.5	4.8	3.8	33.0	4.8	3.8	45.5	7.6	5.7	60.5	5.7	5.7
5	F.field HFT	18.0	12.4	7.6	32.5	5.7	7.6	45.0	4.8	3.8	60.0	4.8	3.8	18.0	7.6	5.7	31.5	6.7	7.6						
6	Compund t. HFT	18.5	9.5	5.7	33.0	5.7	5.7	47.0	4.8	5.7	59.5	8.6	7.6	18.5	6.7	3.8							60.5	6.7	3.8

Figure. 1

Two examples of HFTs, No.3 and No.4. The event No.3 , near- field high-frequency tremor has clear initial phase, and the event No.4 is the seismic-swarm-like near- field high -frequency tremor.

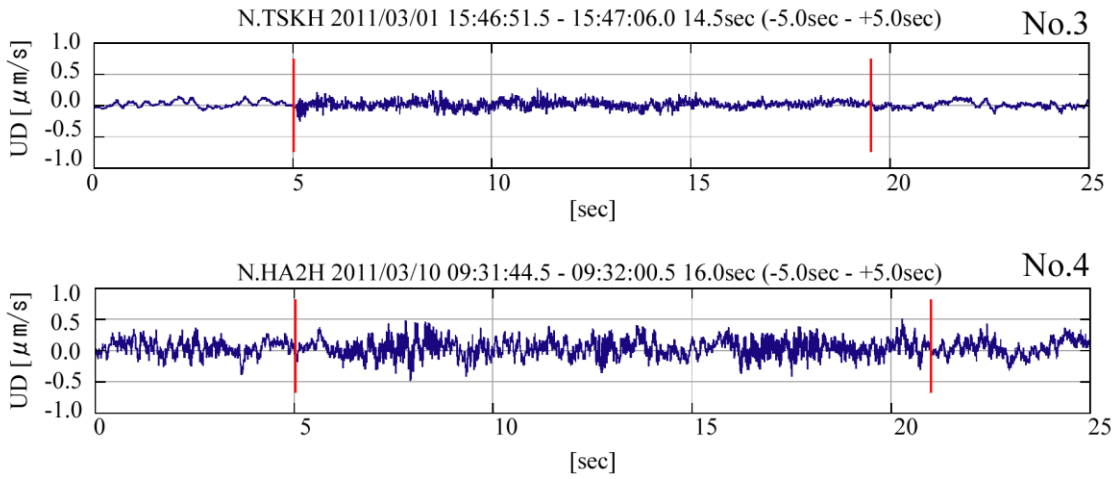

Figure 2. The typical time change of the total score of HFTs No.6 for two months before the Kumamoto earthquake. The event No.6 has very large and isolated peak with the sharpest increase of the total score just before the major earthquake at 21:26 JST on April 16. And there are several peaks with some half total score at other periods.